



# Bioclimatic modelling using Gaussian mixture distributions and multiscale segmentation

Daniel G. Gavin\* and Feng Sheng Hu

Department of Plant Biology, 265 Morrill Hall,  
University of Illinois, Urbana, IL 61801

## ABSTRACT

**Aim** To introduce Gaussian mixture distributions and sequential maximum a posteriori image segmentation (GM-SMAP) as a model that predicts species ranges from mapped climatic variables, and to compare its predictive capacity with two commonly used bioclimatic models: regression tree analysis (RTA) and smoothed response surfaces (SRS).

**Location** North-west North America.

**Methods** We compared models for their ability to predict the distributional range of western hemlock (*Tsuga heterophylla*). We calculated and projected nine climatic and water-balance variables to a 2-km grid up to 140 km from the *T. heterophylla* range. Models were trained using the five variables selected by RTA, as well as subsets of three variables. Goodness of fit was assessed using models trained and tested on the entire study area. Predictive capacity was assessed using 100 cross-validation tests, each trained on a randomly sampled 1% of the study area and tested on the complement of the study area.

**Results** Models using all five variables were significantly better than three-variable models. Model fit was greatest for SRS. GM-SMAP misclassified slightly more area and RTA misclassified almost twice the area compared to SRS. However, cross-validation showed that the predictive capacity was clearly greatest for GM-SMAP and lowest for SRS, indicating that GM-SMAP makes more accurate predictions from sparse data.

**Main conclusions** GM distributions prevent overfitting using an information-theoretic approach, and the SMAP algorithm minimizes the spatial extent of the largest misclassified area using a multiscale method. These properties, useful for image classification, also aid their strong predictive capacity as a bioclimatic model. SRS overfit the data, lowering its predictive capacity, and RTA failed to capture details of interactions among variables, yielding a poor fit. These results demonstrate the strong potential of GM-SMAP as a bioclimatic model.

## Keywords

Actual evapotranspiration, bioclimatic envelope models, ecological niche, model selection, regression tree analysis, response surfaces, *Tsuga heterophylla*, western hemlock.

\*Correspondence: Daniel G. Gavin,  
Department of Plant Biology, 265 Morrill Hall,  
University of Illinois, Urbana, IL 61801.  
E-mail: dgavin@life.uiuc.edu

## INTRODUCTION

Models of the relationship between the observed range of a species and mapped climatic and/or climate-derived variables (ecological niche models or bioclimatic models) are widely used to examine the climatic controls of species range limits and to predict species ranges under future climatic conditions (Scott *et al.*,

2003; Thomas *et al.*, 2004). Although criticized for their simplistic assumption of a strong association between regional climate and species distributions (Loehle & LeBlanc, 1996; Woodward & Beerling, 1997; Hampe, 2004), these models remain useful for understanding the potential for climatic control of range limits and may identify instances where non-climatic factors are important (Pearson & Dawson, 2003; Huntley *et al.*, 2004).

There are many functional forms of bioclimatic models, and the choice of one model over another may have a large effect on the conclusions of a study (Franklin, 1995; Guisan & Zimmermann, 2000; Austin, 2002). However, few studies have compared the strengths and weaknesses of different bioclimatic models (Segurado & Araújo, 2004).

Our overall goal in this study is to demonstrate the performance of an image classification method as a bioclimatic model. This method, introduced by Bouman and Shapiro (1994) and Bouman (1998), first fits a Gaussian mixture distribution to training data and then ‘segments’ maps or images into regions using sequential maximum a posteriori image segmentation (hereafter termed GM-SMAP). The GM-SMAP model was developed primarily for segmenting multiband satellite images into regions with a certain behaviour or spectral signature. Modelling land cover classes using satellite imagery bands is statistically analogous to modelling a species range using mapped climatic variables, though species distribution mapping requires only two classes (species presence and absence). In fact, many models have been used recently for both image segmentation and bioclimatic modelling, including artificial neural networks (Pearson *et al.*, 2002), regression trees (Iverson & Prasad, 2001), generalized additive models (Zaniewski *et al.*, 2002) and genetic algorithms (Oberhauser & Peterson, 2003). Because in remote sensing studies, GM-SMAP outperforms several other methods of image segmentation (McCauley & Engel, 1995; Michelson *et al.*, 2000), we expected that it would be promising as a bioclimatic model.

A key consideration for choosing a bioclimatic model and fitting it to training data is the degree to which the model fits the data structure. If predictor variables have a direct functional control on species presence, then simple thresholds on individual variables could predict species presence. However, it is likely that individual variables alone cannot adequately describe the species–environment relationship, but that variable interactions may approximate an unknown variable with a more direct functional control on the species. Thus, the efficacy of a model depends on how closely it fits the structural complexity of the training data set. Overfitting the training data will result in low predictive capacity, i.e. the ability to predict in regions other than where the model has been trained, and underfitting will not capture meaningful species–environment correlations (Guisan & Zimmerman, 2000). Good fit and predictive capacity are challenging to achieve when using large data sets that capture many details of the species–environment relationship, such as provided by high-resolution maps of large areas. The GM-SMAP model optimizes the fit by using an information-theoretic approach and by mapping predictions in the context of neighbouring grid points. These characteristics are addressed in detail below.

To evaluate the GM-SMAP model, we compare it to two commonly used bioclimatic models: regression tree analysis (RTA) and smoothed response surfaces (SRS). One way to compare these models would be to examine their ability to detect structures in simulated data sets. A recent attempt using this approach to rank 10 multivariate nonparametric regression

models found that it was very difficult to prescribe models for specific data structures (Banks *et al.*, 2003). That study concluded with the recommendation to compare models using a portion of the training data and examining the fit to the ‘holdouts’ (i.e. cross-validation) rather than use arguments based on prior knowledge of the form of the model and the structure of the data. In this study, we follow this recommendation by comparing the capacity of the three models to predict the range of a single species: western hemlock (*Tsuga heterophylla*). By focusing on a single species, we cannot explore the generality of GM-SMAP in other settings. However, *T. heterophylla* serves as a good test case because it is similar to several tree species in the size of its distribution and its juxtaposition with various climatic regions.

We evaluated the three methods for bioclimatic modelling in two steps. First, we trained the models on three sets of bioclimatic variables to evaluate the effects of different variable choices. Model accuracy was assessed by examining the goodness of fit of models trained on the entire study area (resubstitution). Second, we compared the predictive capacity of the models using a cross-validation method where models were trained on random subsamples of the study area and tested on the complement of the study area. The cross-validation analysis is a robust measure of a model’s performance because it demonstrates the capacity to make predictions on new data sets. In contrast, the resubstitution test cannot assess if the model is overfitting the data (Fielding & Bell, 1997).

### The GM-SMAP segmentation model

Modelling species ranges using the GM-SMAP model is a multistep process outlined in Fig. 1. Here we describe these algorithms in non-mathematical intuitive terms; complete formulations are in Bouman and Shapiro (1994) and Bouman (1998). The first step is to fit the training data for two classes (species presence and absence) with a GM distribution using the program CLUSTER

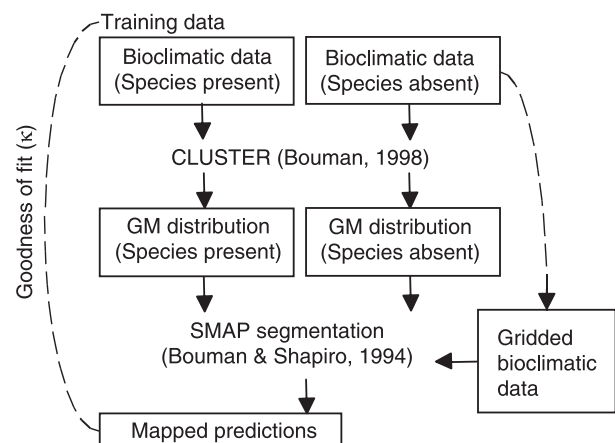


**Figure 1** Steps for predicting species ranges using the Gaussian mixture-sequential maximum a posteriori segmentation (GM-SMAP) model. Dashed lines show the case where predictions are made to the same data used to train the model (resubstitution), with goodness-of-fit summarized by the  $\kappa$  statistic.

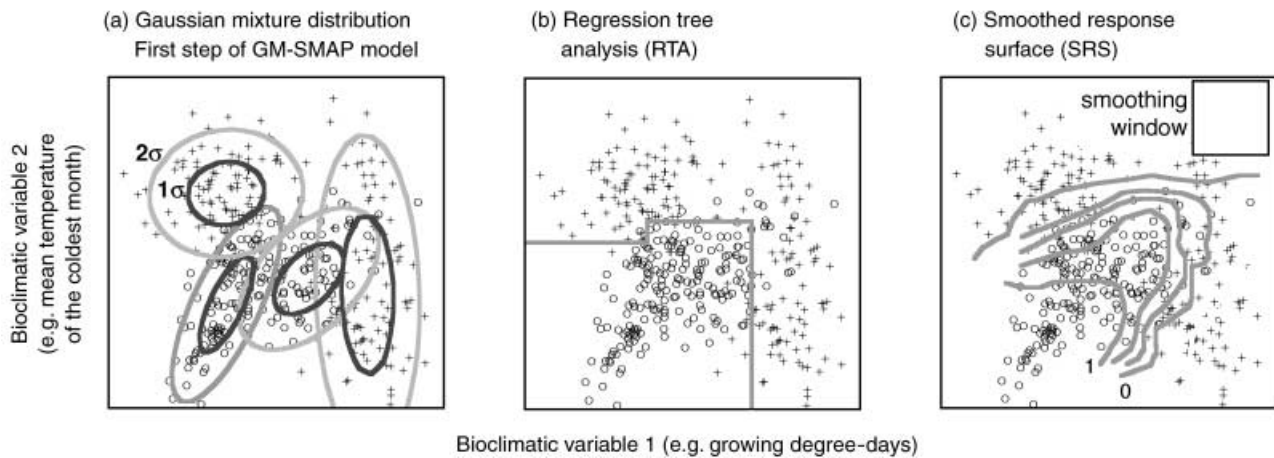


**Figure 2** Schematic representations of the three bioclimatic models used in this paper, simplified in two-dimensional space. Circles and crosses refer to species presence and absence, respectively. (a) Segmentation model that uses the Gaussian mixture distribution of Bouman (1998). Several variance–covariance matrices (shown by ellipses) fit the major form of variation. This ‘climatic signature’ is used with a sequential multiscale a posteriori classification (Bouman & Shapiro, 1994) to classify unknown grid points. (b) Regression tree analysis showing the thresholds (grey lines) of the best-fit regression tree. (c) The smoothed response surface using a tricube centre-weighted filter (Huntley *et al.*, 1989). Contour lines describe the proportion of grid points that are within the species range.

version 3.5.4 (Bouman, 1998). A GM is a probabilistic model composed of a number of subclasses, each described by a multivariate Gaussian distribution (Fig. 2a). Each multivariate Gaussian distribution is defined by a small number of parameters (the mean and variance of each variable, the covariances between each pair of variables, and a weighting based on the proportion of data described by the subclass). While a multivariate Gaussian distribution defines each subclass, the combined mixture of distributions adapts to nonlinear patterns in the data and thus the GM for each class does not resemble a Gaussian distribution. The number of subclasses in the GM can be specified either a priori or estimated directly from the data. The latter approach is appealing because the tightness of the fit of the GM can be determined objectively to avoid overfitting or underfitting as described below.

The GM distribution is fit by first initializing a large number of subclasses with the means, covariances and ‘weightings’ of each subclass. This ‘seed’ GM is made of randomly selected means and identical variance-covariance matrices based on the entire data set. Subclasses are then modified using the iterative expectation maximization (EM) algorithm of Dempster *et al.* (1977). This algorithm (1) estimates the probability of each observation in the training data belonging to each subclass (using the GM parameters) then (2) re-computes the maximum-likelihood estimate of the GM parameters using the probabilities from step 1. These two steps are repeated until the GM parameters converge on a final maximum-likelihood estimate.

The steps described above computes a GM for a predetermined number of subclasses, but they do not address how to determine the ‘best’ number of subclasses in a GM. Adding more subclasses always increases the fit of the GM, but too many subclasses would record fine-scale structures in the data resulting in overfitting. The CLUSTER program guards against overfitting by using the minimum description length (MDL) estimator (Grünwald,

2004), a selection method that weighs complexity in the model against complexity in the data. MDL is calculated by penalizing the maximum likelihood of the model with increases in the number of model parameters and the sample size (Bouman, 1998). This procedure prevents models from adding more subclasses when the additional complexity yields diminishing returns in increased fit. As applied here, MDL is used to compare the fit of GM distributions composed of different numbers of subclasses. The number of subclasses is reduced from the initial large number by combining the two nearest subclasses and running the EM algorithm on the new set of subclasses. This agglomeration of subclasses is repeated until only one subclass remains, and the number of subclasses retained in the final GM is the one with the smallest MDL.

Predictions from the GM distribution are projected onto mapped variables using the sequential maximum a posteriori (SMAP) algorithm, available in GRASS GIS software (Bouman & Shapiro, 1994). This Bayesian approach is a type of Markov chain model applied across resolutions or scales. The SMAP algorithm segments grid-point class labels (i.e. species presence or absence) at multiple resolutions using (1) the class label at the previous coarser resolution, (2) the GM distribution, and (3) a cost function. The cost function, a measure of the probability of a coarse-resolution label changing at finer resolutions, is calibrated by a fine-to-coarse procedure in which class labels at each resolution are compared to the data at finer resolutions. The cost function puts exponentially greater weight on errors at coarse resolutions because those errors correspond to larger areas. Both the fine-to-coarse cost function calibration and the coarse-to-fine segmentation are applied to the gridded variables using a structure that defines the neighbour relationships across resolutions (Fig. 3). At fine resolutions, this structure is a quadtree, and each grid point depends on one coarse-resolution neighbour (Fig. 3a). If applied to coarse resolutions, the quadtree structure would

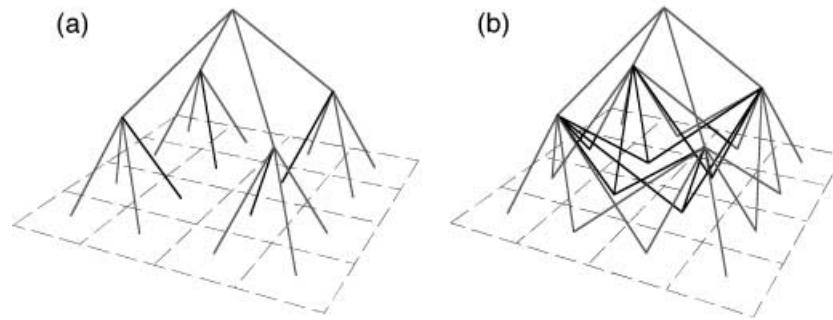


**Figure 3** Spatial structure of relationships across multiple resolutions used in the SMAP algorithm. Figure modified from Bouman and Shapiro (1994). (a) The quadtree structure used at fine resolutions. The dashed lines represent the gridded data at the finest resolution. The black lines show the connection of grid points to their coarse-scale neighbours for the four central grid points. The grey and black lines together show the scheme for merging grid points to compute coarse-resolution grids. (b) The augmented pyramidal structure used at coarse resolutions. Note that the central four grid points each have three coarse-resolution neighbours.

result in unrealistically blocky regions. Thus, at coarse resolutions, the quadtree structure is replaced by an augmented pyramidal structure in which each grid point is dependent on three coarse-resolution neighbours (Fig. 3b). This structure results in smooth region boundaries during the coarse-to-fine segmentation. Details of these calculations are presented in Bouman and Shapiro (1994) and software for CLUSTER and SMAP is freely available (<http://www.ece.purdue.edu/~bouman>).

The net effect of the SMAP algorithm is to make a more spatially contiguous classification than would be achieved if each grid point were classified independently using a maximum-likelihood method. The cost function adapts to the scale of heterogeneity (patchiness) in the data, and thus does not overly smooth classifications. Therefore, SMAP maximizes the accuracy of predictions by minimizing the size of the largest misclassified region and creating predictions with the level of spatial autocorrelation that occurs in species range maps.

## METHODS

### Zonal ecosystems and bioclimatic variables

We trained models on zonal ecosystems with *T. heterophylla* as a dominant species. Zonal ecosystems, sometimes termed biogeoclimatic zones, are defined as areas with relatively homogeneous late successional vegetation in the absence of local controls, such as atypical soil or drainage (Meidinger & Pojar, 1991). Models trained on zonal ecosystem capture regional-scale bioclimatic variations that define the zonal ecosystem. The perimeter of all known occurrences of a species based on actual (plot-based) observations is less appropriate because it encompasses diffuse range limits where microclimates differ from the regional climate and where biotic interactions may be strong. Zonal ecosystems are mapped by interpolating between field plots using locally derived elevation and aspect rules, and thus can capture elevationally stratified forest zones at scales of < 500 m (Meidinger & Pojar, 1991). To create a 2-km resolution *T. heterophylla* map, we merged four widely

used ecosystem classifications developed by various government agencies:

- (1) Broad Ecosystem Inventory by the British Columbia Ministry of Sustainable Resource Management, covering British Columbia, southeast Alaska, Washington and Idaho (85.2% of the *T. heterophylla* zone; <http://www.gov.bc.ca/ecology/bei/shiningmntns.html>)
- (2) Ecoregions of Oregon by the United States Geological Survey (13.7%; <http://www.gis.state.or.us/data/alphalist.html>)
- (3) Alaska Statewide Vegetation by the United States Geological Survey (0.7%; <http://agdc.usgs.gov/data/projects/hlct/hlct.html>)
- (4) California Vegetation Maps by the United States Forest Service (0.4%; <http://gis.ca.gov/catalog/BrowseRecord.epl?id=708>).

Climatic and water-balance variables were developed from the monthly normals available from the PRISM climate mapping project (Daly *et al.*, 1994). These peer-reviewed maps were created by interpolating weather station data with elevation as a covariate and with algorithms to estimate rain shadow effects, thermal inversions and coastal climates. We initially examined nine potential bioclimatic variables (Table 1), focusing on summer moisture stress, which is a known physiological limit on the *T. heterophylla* range (Waring & Franklin, 1979; Lassoie *et al.*, 1986). Potential annual evapotranspiration (PET) and actual annual evapotranspiration (AET) were estimated using the water-balance model presented in Willmott *et al.* (1985). All climatic variables and the water-balance model were calculated for each 2-km grid point. The maximum correlation coefficient was 0.66 between any pair of variables. We did not include the annual climatic moisture deficit (PET-AET; Stephenson, 1998) because it was highly correlated ( $r = 0.98$ ) with the widely used AET/PET moisture index (Huntley *et al.*, 1995).

### RTA and SRS bioclimatic models

We compared model predictions from the GM-SMAP model (described above) to regression tree analysis (RTA) and smoothed response surfaces (SRS). The RTA model classifies grid points using a branching decision tree (identical to classification and

**Table 1** Climatic and water-balance variables assessed for use with bioclimatic modelling of the *Tsuga heterophylla* zone

Variable	Code	2.5th–97.5th percentiles ( <i>T. heterophylla</i> zone and total region)*	Window width for response surfaces†
Mean temperature of the coldest month (°C)	MTCO	–10.8–5.5 –20.2–4.5	4.0
Growing degree-days on a 5° base‡	GDD5	515–2425 107–2511	400
Actual annual evapotranspiration (mm)§	AET	384–608 238–580	40
Moisture index	AET/PET	0.699–0.995 0.398–0.995	0.05
Annual precipitation (mm)	P	650–4930 225–5073	
Effective precipitation (mm)	P-PET	145–4418 –320–4621	800
July precipitation (mm)	P07	11–20 4–250	
Snow water equivalent (mm)¶	SWE	0–1704 0–2635	
Minimum monthly humidity index**	P/PET	0.14–2.00 0.06–2.07	

\*The percentile from within the *Tsuga heterophylla* zone may exceed that for the entire region if *T. heterophylla* is clustered at one end of the gradient.

†The window width is a value used to create smoothed response surfaces. It is only given for variables used in the response surface analysis.

‡Calculated by interpolating monthly values.

§The water balance was modelled using a custom-written program, following Willmott *et al.* (1985). We assumed a uniform soil field capacity of 100 mm, and day length calculations followed Forsythe *et al.* (1995).

¶Sum of precipitation on months with mean temperature < –1 °C.

\*\*The month with the lowest P/PET.

regression trees, CART; Iverson & Prasad, 2001). It was run using R software integrated with GRASS GIS (Therneau & Atkinson, 1997) following the methods of Breiman *et al.* (1984). Each split in the decision tree represents the threshold of the variable from a large list of candidate variables (Table 1) that most accurately classifies grid points. This results in a set of thresholds for each variable that are dependent on values of other variables (Fig. 2b). For this study, the regression tree was grown until further branching did not improve the overall classification better than 0.25%, and then the tree was pruned back by using a cross-validation method to remove spurious branching (Breiman *et al.*, 1984).

The SRS model develops a response surface based on the relative frequency of grid points with species present vs. absent in climate space (Huntley *et al.*, 1989). Our use of SRS (using a custom computer program) is similar to locally weighted regression (LOESS) and nonparametric multiplicative regression presented in McCune *et al.* (2003). Rather than developing a response surface on an arbitrary lattice within climate space and making predictions from values in this lattice, we calculated the exact response surface value for each grid point to be predicted. For each grid point, the number of additional grid points within a specific climatic window was calculated. The window width of

each variable was approximately 20% of the central 95% range within the *T. heterophylla* zone (Table 1). Each point falling within this window was weighted using the tricube filter (Huntley *et al.*, 1989), so that grid points with a very similar climate were weighted more heavily than points closer to the limits of the window (Fig. 2c). The same weighted sum was calculated both for the points within the *T. heterophylla* zone and for all points within and outside the *T. heterophylla* zone. The response surface value was calculated as the ratio of these two values, and ranged between 0 (climate at the grid point is unlike any in the *T. heterophylla* zone) to 1 (climate at the grid point is unlike any *not* in the *T. heterophylla* zone). Thresholds for determining *T. heterophylla* presence were set where the underprediction (omission) error rate was at least as low as for other models and lower than the overprediction (commission) error rate.

### Modelling strategy

As GM-SMAP and SRS do not automatically determine which variables to include in the model, we compared model fits using three sets of climatic variables. The first set of variables is widely used in other modelling studies (e.g. Huntley *et al.*, 1995; Shafer *et al.*, 2001): AET/PET (actual/potential annual evapotranspiration),

GDD5 (growing degree days on a 5 °C base) and MTCO (mean temperature of the coldest month). The other two sets of variables were the best three (AET, MTCO and AET/PET) and the best five (AET MTCO AET/PET GDD5 and P-PET: effective precipitation) variables identified by RTA. To make the calculations tractable, we limited the study area to the *T. heterophylla* zone plus 140 km immediately outside the zone, a distance chosen to encompass the area between the interior and coastal portions of the zone ( $n = 75,502$  and  $292,124$  grid points within and outside of the *T. heterophylla* zone, respectively). Note that grid points correspond to the ecosystem-level map we used to infer presence and absence rather than actual presence/absence observations.

Goodness of fit of each model was assessed by comparing the predicted to the observed zone using the  $\kappa$  (kappa) statistic, a measure of the accuracy of a classification. We chose to use  $\kappa$  because the response variables of RTA and GM-SMAP are not continuous, precluding threshold-independent methods such as the receiver-operating characteristic (ROC plots; Fielding & Bell, 1997).  $\kappa$  is calculated as  $[Po - Pe] / [1 - Pe]$ , where  $Po$  is the proportion of grid points that agree between the predicted and observed zones and  $Pe$  is the proportion of grid points expected to agree by chance.  $\kappa$  ranges from  $-1$  (the predicted and observed ranges are mirror images of each other) to  $1$  (the predicted zone exactly matches the observed zone). Estimating confidence intervals (CIs) of  $\kappa$  was difficult because of spatial autocorrelation and the fact that the large number of grid points unrealistically reduced the variance in  $\kappa$ . We estimated the 95% CI of  $\kappa$  to be  $c. \pm 0.02$  following Fleiss *et al.* (1969) after reducing the sample size to account for the fact that most spatial autocorrelation occurs at a scale of 10 km. Because of the problems with determining a CI, we compared  $\kappa$ -values cautiously.

The predictive capacities of the models were compared using a cross-validation procedure where the study area was divided into training data and testing data. Some studies have employed a leave-one-out cross-validation where one grid point is predicted based on a model trained on all other grid points (McCune *et al.*, 2003). However, the fine spatial resolution and strong autocorrelation in the climatic data suggest that a leave-one-out cross validation would differ little from the model trained on the entire study area, and thus not adequately evaluate predictive capacity. We used a  $k$ -fold cross-validation strategy (Fielding & Bell, 1998) that more thoroughly evaluates predictive capacity by training models on small spatially stratified random subsamples. It involved training each of the three models on 100 sets of 1% subsamples (i.e. 3660 grid points) and computing  $\kappa$  on predictions made to the complement (99%) of grid points. This small, yet very representative, subsample was chosen as a rigorous test of the capacity of a model to predict in climates differing slightly from the training set. Grid points in each subsample were spaced  $\geq 20$  km to assure equal representation of the entire map and reduce autocorrelation among subsampled grid points. A model with good predictive capacity would have a consistently high cross-validation  $\kappa$ .

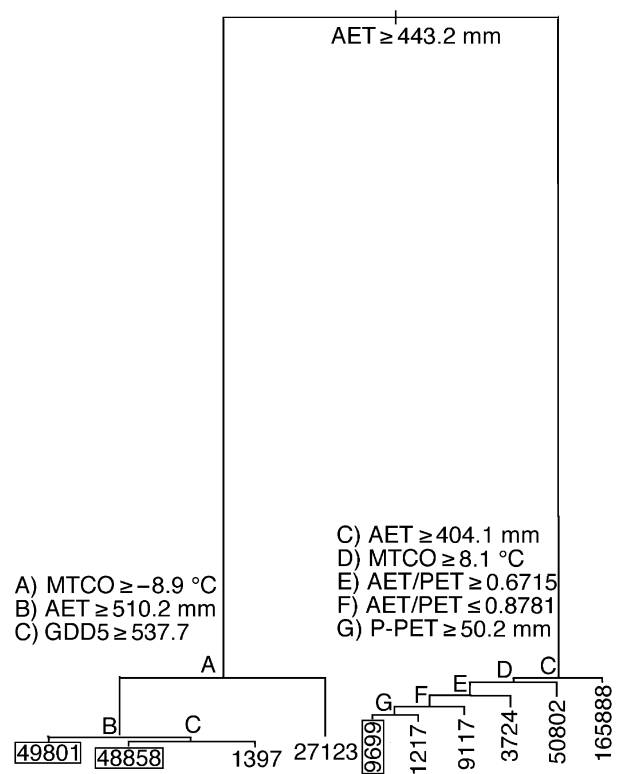


**Figure 4** Regression tree predicting the *Tsuga heterophylla* zone. The number of grid points is shown at each terminal leaf. Numbers in boxes indicate leaves classified as the *T. heterophylla* zone. The vertical distance between nodes is proportional to the percentage of the data explained by each split.

**RESULTS**

The regression tree shows that AET is the single most important variable at determining the *T. heterophylla* zone (Fig. 4). A single threshold of 443 mm correctly classifies 78.6% of the grid points, and adding MTCO and AET/PET increases the total percentage correctly classified to 84.0%. Two additional variables (GDD5 and P-PET) result in a marginal improvement (84.6%). No other variables meet the criteria of increasing the accuracy by 0.25%. The accuracy is much higher for low AET (outside the *T. heterophylla* zone) than for high AET (94.4% and 48.8%, respectively). Where  $AET \leq 443$  mm, adding five branches based on three additional variables (MTCO, AET/PET and P-PET) only increases accuracy slightly both within and outside the *T. heterophylla* zone. Where  $AET > 443$  mm, adding a branch at an MTCO of  $-8.9$  °C increases the accuracy to 66.4%, but further branching involving AET and GDD5 only marginally increases accuracy on this side of the tree.

Of the variable sets, the five-variable set fits the observed *T. heterophylla* zone significantly better than either three-variable set for the GM-SMAP and SRS models (Table 2). The increase in  $\kappa$  between these variable sets is 0.051 and 0.074 for GM-SMAP and SRS, respectively, which exceeds the estimated  $\kappa$  CI of  $\pm 0.02$  (see Methods). For RTA,  $\kappa$  increases only 0.024 between these variable sets, consistent with this model’s small increase in

**Table 2** Results of resubstitution tests of three bioclimatic models predicting the *Tsuga heterophylla* zone

Model	Variable set	Percent underprediction	Percent overprediction	$\kappa$
GM-SMAP	GDD5, MTCO, AET/PET	18.0	18.4	0.532
	AET, MTCO, AET/PET	15.2	15.7	0.592
	AET, MTCO, AET/PET, GDD5, P-PET	9.3	14.0	0.643
RTA	GDD5, MTCO, AET/PET	13.8	19.1	0.548
	AET, MTCO, AET/PET	15.5	16.1	0.581
	AET, MTCO, AET/PET, GDD5, P-PET	18.9	13.3	0.605
SRS	GDD5, MTCO, AET/PET	13.5	14.8	0.629
	AET, MTCO, AET/PET	12.8	14.7	0.641
	AET, MTCO, AET/PET, GDD5, P-PET	8.3	11.1	0.715

AET/PET = actual/potential annual evapotranspiration, GDD5 = growing degree-days on a 5 °C base, MTCO = mean temperature of the coldest month and P-PET = effective precipitation.

overall accuracy because of increased branching (Fig. 4). All models using the three best variables identified by RTA (AET, MTCO and AET/PET) have a better fit than the commonly used three-variable set (GDD5, MTCO and AET/PET), with  $\kappa$  differences of 0.012–0.060.

Of the three models using the five-variable set, SRS has the closest fit, and GM-SMAP has a better fit than RTA (Table 2). The improved fit of SRS over GM-SMAP (difference in  $\kappa = 0.072$  for the five-variable set) is twice that for GM-SMAP over RTA (difference in  $\kappa = 0.038$ ). The poorer fit of GM-SMAP is because of a 2.9% greater overprediction compared to SRS (Table 2). GM-SMAP and SRS overpredict in the same areas (blue areas on Fig. 5), but these areas are more contiguous in the GM-SMAP model and thus cover a larger area. In contrast, the poorer fit of

RTA is because of a *c.* 9% greater underprediction compared to the other models. This underprediction occurs mainly in the northern valleys in the interior portion of the *T. heterophylla* zone (Fig. 5). All models overpredict in high elevation coastal areas of British Columbia and southeast Alaska with very steep terrain, and in the south-eastern portion of the interior range of *T. heterophylla*.

Cross-validation tests show that GM-SMAP has the greatest predictive capacity of the three models (Fig. 6). The median  $\kappa$  of 100 cross-validation tests is significantly greater for GM-SMAP (0.555) than for RTA (0.526) or SRS (0.480). The decrease in  $\kappa$  between models trained on the full study area and on 1% of the study area (cross validation) is much greater for SRS (0.235) than for RTA (0.079) or GM-SMAP (0.088).

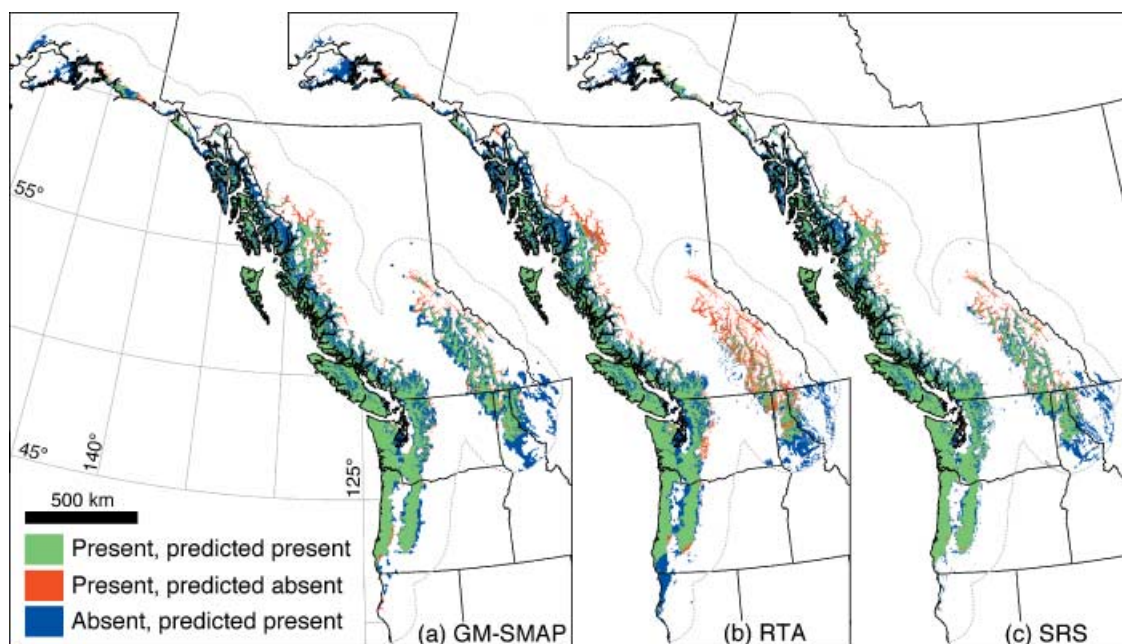


**Figure 5** Model predictions for the three bioclimatic models. The dashed line indicates the area within 140 km of the *T. heterophylla* range where bioclimatic models were trained and applied. All models were based on five climatic or water-balance variables (Table 2). The projection is Albers Equal Area, centred on British Columbia.

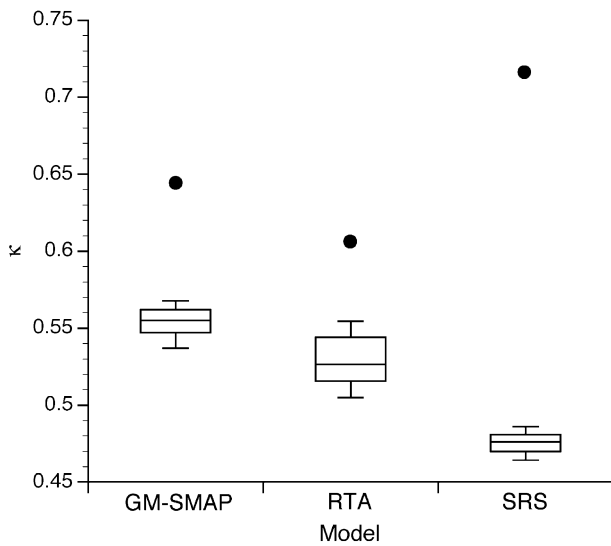


**Figure 6** Cross-validation results for three bioclimatic models. Circles are the  $\kappa$  statistics for models trained on, and applied to, the entire study area (Table 2). The box plot shows the range of  $\kappa$  statistics for models trained on 100 random subsamples of 1% of the grid points and applied to the complement of grid points. The box indicates the 25th and 75th percentiles (the centre line is the median), and the lines indicate the 10th and 90th percentiles.

Examples of mapped cross-validation predictions show spatial patterns of prediction error (Fig. 7). All models greatly overpredict areas surrounding the interior portion of the *T. heterophylla* zone. SRS has the greatest overprediction, with much fine-scale variability, and it also underpredicts a large area in western Washington and Oregon. GM-SMAP and RTA show more contiguous patterns in overpredicted areas. The areas of overprediction are generally smaller for GM-SMAP than for RTA but the locations are similar.

## DISCUSSION

### Selection of climatic variables for species range prediction

RTA identified AET as the most predictive variable. Along with the climatic water deficit (which was highly correlated with AET/PET), AET has been shown to be a superior predictor of vegetation from local species distributions to biomes (Stephenson, 1998). AET integrates growing season temperature and available moisture (i.e. biologically available energy and water), and thus, species with different moisture and energy requirements should be patterned along the AET gradient. *T. heterophylla* is a species with one of the highest moisture requirements among conifers (Lassoie *et al.*, 1986), hence its occurrence at high AET. In contrast, the variable set commonly used in bioclimatic models replaces AET with GDD5 (Table 2), which does not capture the interaction of energy and water availability (Stephenson, 1998). For *T. heterophylla*, this variable set performed poorly when compared with the best three or five variables identified by RTA, regardless of the model form (Table 2). These results demonstrate that RTA or other models that select among candidate variables (e.g. logistic regression) can be used to identify biologically meaningful variables for models that lack this capacity (Walker & Cocks, 1991). There is no automated method for selecting variables in SRS and GM-SMAP, and the alternative of comparing resubstitution and cross-validation results of all variable combinations would be an overwhelming task for large data sets.

Models using five variables were a large improvement over those using three variables, justifying the increased complexity of the two additional variables. This improvement was especially large for GM-SMAP and SRS whose fits increased two to three times more than that of RTA (Table 2). It is likely that GM-SMAP

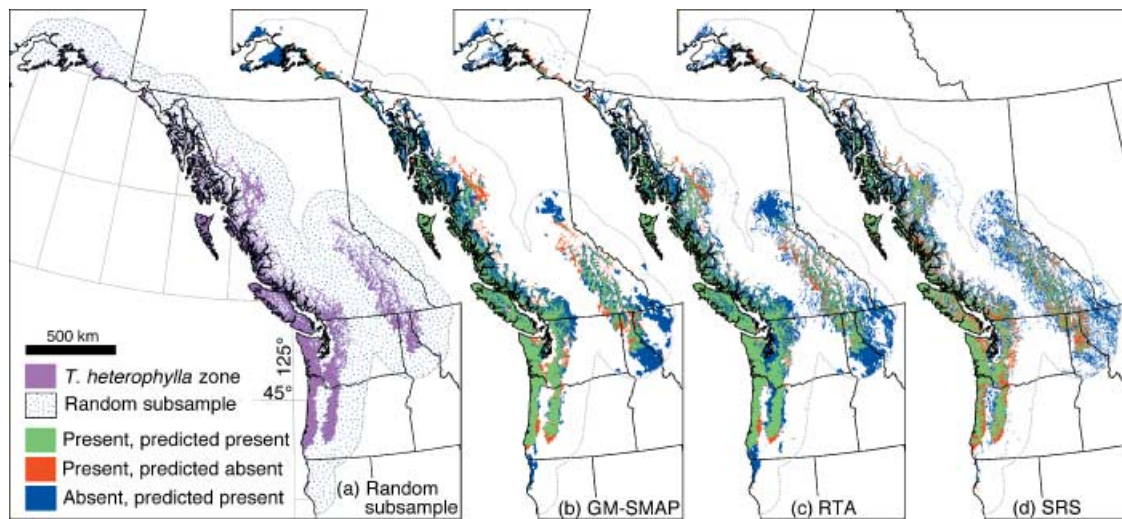


**Figure 7** Example of one typical cross-validation model. (a) A spatially stratified random subsample of 1% of the study area used to train each model. (b–d) Predictions from models trained on the subsample in (a).

**Table 3** Number of subclasses identified for the Gaussian mixture distributions

Variable set	Class	
	Within <i>T. heterophylla</i> zone ( <i>n</i> = 75,502 grid points)	Outside <i>T. heterophylla</i> zone ( <i>n</i> = 292,124 grid points)
GDD5, MTCO, AET/PET	22	58
AET, MTCO, AET/PET	37	44
AET, MTCO, AET/PET, GDD5, P-PET	61	88

AET/PET = actual/potential annual evapotranspiration, GDD5 = growing degree-days on a 5 °C base, MTCO = mean temperature of the coldest month and P-PET = effective precipitation.

and SRS captured variable interactions better than RTA (Fig. 2). For example, the Gaussian mixture identified about twice the number of subclasses for the five-variable vs. three-variable sets (Table 3). In addition, for both GM-SMAP and SRS, five variables resulted in a smaller amount of underprediction than three variables (Table 2). Underprediction is likely a failure of the model algorithm, as it indicates that the model cannot predict areas where a species is known to occur. Overprediction, on the other hand, can have plausible ecological explanations (e.g. slow migration rates or interspecific competition) and thus is not as serious an error as underprediction (Svenning & Skov, 2004). The ecological interpretation of non-climatic factors affecting overprediction of *T. heterophylla* is the focus of another study (Gavin & Hu, unpublished data).

### Comparisons of bioclimatic models

Of the three models, GM-SMAP had the greatest predictive capacity (as determined by cross validation), which we attribute to the GM distribution for summarizing climatic relationships and the multiscale SMAP algorithm for making predictions. The GM distribution uses objective criteria (the MDL) to automatically determine the appropriate level of generalization (Grünwald, 2004). In contrast, RTA may be too general, not capturing the complexity of variable interactions because thresholds were based on a small number of perpendicular planes. On the other hand, SRS may be too specific, using a uniform climatic window that required enough data within the window to make a prediction. An advantage of the GM is that it includes variable interactions (using a variance–covariance matrix for each subclass) and adapts to sharp or diffuse transitions of species abundance on climatic gradients. The latter property means that GMs can identify abrupt climatic thresholds but also interpolate across poorly sampled regions in climate space in the same model (Fig. 2a). For example, the GM identified 61 subclasses when trained on the *T. heterophylla* zone over the entire study area (Table 3), and an average of five subclasses when trained on cross-validation subsamples. The smaller number of subclasses for the smaller cross-validation subsamples indicated greater generalization and interpolation within climate space when using sparser data. We suggest that this adaptability of the GM method increased the predictive capacity of GM-SMAP relative to RTA and SRS.

The use of the MDL in the GM fitting algorithm is highly suitable for predictive modelling of species ranges as it automates

model selection, resulting in the ‘best’ model as a trade-off between fit and generalization (Rushton *et al.*, 2004). The MDL or other information-theoretic approaches [e.g. the Akaike Information Criteria (AIC) Burnham & Anderson, 2002] can be used not only to parameterize models of a particular form (e.g. GM distributions), but also to compare models with diverse forms. However, because SRS, as applied in this study, is a smoother of the data instead of a parameterized model (see below), it could not be described by such criteria. Therefore, we relied on cross validation as a practical demonstration of a model’s robustness and ability to predict in areas outside the training data set.

GM-SMAP makes predictions from the GM ‘signature’ using a multiscale algorithm (SMAP) that classifies each grid point in the context of the climate of neighbouring points, minimizing prediction of small outlier areas. SMAP increased the  $\kappa$  of cross-validation tests by an average of 0.015 when compared to a point-by-point maximum likelihood method (not shown) that used the same GM distribution. Thus, the SMAP algorithm was partly responsible for the improved fit of GM-SMAP over RTA and SRS in cross-validation (difference in  $\kappa$  *c.* 0.03 and 0.075, respectively; Fig. 6). In contrast, the spatially unrealistic SRS cross-validation result (Fig. 7) may be partly due to predictions in each grid point made independently of the neighbouring grid points. Similarly, improved fit because of the SMAP algorithm has been found in remote sensing studies where it outperformed maximum-likelihood classification (McCaughey & Engel, 1995) and artificial neural networks (Michelson *et al.*, 2000).

In contrast to RTA and GM-SMAP, SRS has no automated method to guard against overfitting, and the method is difficult to implement. SRS is better described as a ‘smoother’ than as a statistical model because it does not generalize the training data into a compressed format. The entire training data set is required to make each prediction, requiring long computer run times. This lack of generalization makes it difficult to use a selection method such as MDL to aid model selection (e.g. window width of the smoothing function). Instead, the window width used in SRS is set a priori, and determining the optimal window for each variable via an iterative trial-and-error procedure would be prohibitive for large data sets. In this study, the window size (20% of the central 95% range of each variable) was likely too specific. These issues highlight a significant advantage of the GM-SMAP model: no subjective decisions are required once the predictor variables are chosen.

The characteristics of the GM-SMAP model and its capacity to predict *T. heterophylla* suggest that it performs well in other settings. However, several other recently introduced models may perform equally well. For example, multivariate adaptive regression splines (MARS) and general additive models (GAM) are similar to or more competitive than RTA (Prasad & Iverson, 2000; Moisen & Frescino, 2002; Banks *et al.*, 2003; Munoz & Felicísimo, 2004). MARS appears to be superior to many models at fitting data where only a portion of the variables is explanatory (Banks *et al.*, 2003), and artificial neural networks are very predictive, though dependent on the characteristics of the species distribution (Segurado & Araujo, 2004). Further evaluation of GM-SMAP should include comparisons with these models and with a variety of training data sets.

## ACKNOWLEDGEMENTS

This research was funded by the US National Science Foundation (DEB 02-12917) and the Packard Foundation. The authors thank two anonymous reviewers for comments on the manuscript.

## REFERENCES

- Austin, M.P. (2002) Spatial prediction of species distribution: an interface between ecological theory and statistical modelling. *Ecological Modelling*, **157**, 101–118.
- Banks, D.L., Olszewski, R.T. & Maxion, R.A. (2003) Comparing methods for multivariate nonparametric regression. *Communications in Statistics — Simulation and Computation*, **32**, 541–571.
- Bouman, C.A. (1998) *CLUSTER: an unsupervised algorithm for modeling Gaussian mixtures*. Online manual. <http://www.ece.purdue.edu/~bouman>. [Accessed 1 October 2004]
- Bouman, C.A. & Shapiro, M. (1994) A multiscale random-field model for Bayesian image segmentation. *IEEE Transactions on Image Processing*, **3**, 162–177.
- Breiman, L., Friedman, J., Olshen, R. & Stone, C. (1984) *Classification and regression trees*. Wadsworth, Belmont, California.
- Burnham, K.P. & Anderson, D.R. (2002) *Model selection and multi-model inference: a practical information-theoretic approach*. Springer, New York.
- Daly, C., Neilson, R.P. & Phillips, D.L. (1994) A statistical-topographic model for mapping climatological precipitation over mountainous terrain. *Journal of Applied Meteorology*, **33**, 140–158.
- Dempster, A., Laird, N. & Rubin, D. (1977) Maximum likelihood from incomplete data via the EM algorithm. *Journal of the Royal Statistical Society B*, **39**, 1–38.
- Fielding, A.H. & Bell, J.F. (1997) A review of methods for the assessment of prediction errors in conservation presence/absence models. *Environmental Conservation*, **24**, 38–49.
- Fleiss, J.L., Cohen, J. & Everitt, B.S. (1969) Large-sample standard errors of kappa and weighted kappa. *Psychological Bulletin*, **72**, 323–327.
- Forsythe, W.C., Rykiel, E.J. Jr, Stahl, R.S., Wu, H. & Schoolfield, R.M. (1995) A model comparison for daylength as a function of latitude and day of year. *Ecological Modelling*, **80**, 87–95.
- Franklin, J. (1995) Predictive vegetation mapping: geographic modelling of biospatial patterns in relation to environmental gradients. *Progress in Physical Geography*, **19**, 474–499.
- Grünwald, P. (2004) A tutorial introduction to the minimum description length principle. *Advances in minimum description length: theory and applications* (ed. by P. Grünwald, I. J. Myung and M. Pitt), MIT Press, Cambridge, MA.
- Guisan, A. & Zimmermann, N.E. (2000) Predictive habitat distribution models in ecology. *Ecological Modelling*, **135**, 147–186.
- Hampe, A. (2004) Bioclimatic envelope models: what they detect and what they hide. *Global Ecology and Biogeography*, **13**, 469–471.
- Huntley, B., Bartlein, P.J. & Prentice, I.C. (1989) Climatic control of the distribution and abundance of beech (*Fagus L.*) in Europe and North America. *Journal of Biogeography*, **16**, 551–560.
- Huntley, B., Berry, P.M., Cramer, W. & McDonald, A.P. (1995) Modelling present and potential future ranges of some European higher plants using climate response surfaces. *Journal of Biogeography*, **22**, 967–1001.
- Huntley, B., Green, R.E., Collingham, Y.C., Hill, J.K., Willis, S.G., Bartlein, P.J., Cramer, W., Hagemeyer, W.J.M. & Thomas, C.J. (2004) The performance of models relating species geographical distributions to climate is independent of trophic level. *Ecology Letters*, **7**, 417–426.
- Iverson, L.R. & Prasad, A.M. (2001) Potential changes in tree species richness and forest community types following climate change. *Ecosystems*, **4**, 186–199.
- Lassoie, J.P., Hinckley, T.M. & Grier, C.C. (1986) Coniferous forests of the Pacific Northwest. *Physiological ecology of North American plant communities* (ed. by B.F. Chabot and H.A. Mooney), pp. 127–161. Chapman & Hall, New York.
- Loehle, C. & LeBlanc, D. (1996) Model-based assessments of climate change effects on forests: a critical review. *Ecological Modelling*, **90**, 1–31.
- McCauley, J.D. & Engel, B.A. (1995) Comparison of scene segmentations: SMAP, ECHO, and maximum likelihood. *IEEE Transactions on Geoscience and Remote Sensing*, **33**, 1313–1316.
- McCune, B., Berryman, S.D., Cissel, J.H. & Gitelman, A.I. (2003) Use of a smoother to forecast occurrence of epiphytic lichens under alternative forest management plans. *Ecological Applications*, **13**, 1110–1123.
- Meidinger, D. & Pojar, J. (1991) *Ecosystems of British Columbia. Special Report Series no. 6*. British Columbia Ministry of Forests, Research Branch, Victoria, BC.
- Michelson, D.B., Liljeberg, B.M. & Pilesjö, P. (2000) Comparison of algorithms for classifying Swedish landcover using Landsat TM and ERS-1 SAR data. *Remote Sensing of Environment*, **71**, 1–15.
- Moisen, G.G. & Frescino, T.S. (2002) Comparing five modelling techniques for predicting forest characteristics. *Ecological Modelling*, **157**, 209–225.
- Munoz, J. & Felicísimo, A.M. (2004) Comparison of statistical methods commonly used in predictive modelling. *Journal of Vegetation Science*, **15**, 285–292.

- Oberhauser, K. & Peterson, A.T. (2003) Modeling current and future potential wintering distributions of eastern North American monarch butterflies. *Proceedings of the National Academy of Sciences of the United States of America*, **100**, 14063–14068.
- Pearson, R.G. & Dawson, T.P. (2003) Predicting the impacts of climate change on the distribution of species: are bioclimate envelope models useful? *Global Ecology and Biogeography*, **12**, 361–371.
- Pearson, R.G., Dawson, T.P., Berry, P.M. & Harrison, P.A. (2002) SPECIES: a spatial evaluation of climate impact on the envelope of species. *Ecological Modelling*, **154**, 289–300.
- Prasad, A.M. & Iverson, L.R. (2000) Predictive vegetation mapping using a custom built model-chooser: comparison of Regression Tree Analysis and Multivariate Adaptive Regression Splines. *4th International Conference on Integrating GIS and Environmental Modeling (GIS/EM4): Problems, Prospects and Research Needs*. Banff, Alberta, Canada.
- Rushton, S.P., Ormerod, S.J. & Kerby, G. (2004) New paradigms for modelling species distributions? *Journal of Applied Ecology*, **41**, 193–200.
- Scott, J.M., Heglund, P.J., Morrison, M.L., Haufler, J.B., Raphael, M.G., Wall, W.A. & Samson, F.B., eds. (2003) *Predicting species occurrences: issues of accuracy and scale*. Island Press, Washington.
- Segurado, P. & Araújo, M.B. (2004) An evaluation of methods for modelling species distributions. *Journal of Biogeography*, **31**, 1555–1568.
- Shafer, S.L., Bartlein, P.J. & Thompson, R.S. (2001) Potential changes in the distributions of western North America tree and shrub taxa under future climate scenarios. *Ecosystems*, **4**, 200–215.
- Stephenson, N.L. (1998) Actual evapotranspiration and deficit: biologically meaningful correlates of vegetation distribution across spatial scales. *Journal of Biogeography*, **25**, 855–870.
- Svenning, J.C. & Skov, F. (2004) Limited filling of the potential range in European tree species. *Ecology Letters*, **7**, 565–573.
- Therneau, T.M. & Atkinson, E.J. (1997) *An introduction to recursive partitioning using the RPART routines*. Department of Health Science Research, Mayo Clinic, Rochester, Minnesota.
- Thomas, C.D., Cameron, A., Green, R.E., Bakkenes, M., Beaumont, L.J., Collingham, Y.C., Erasmus, B.F.N., de Siqueira, M.F., Grainger, A., Hannah, L., Hughes, L., Huntley, B., van Jaarsveld, A.S., Midgley, G.F., Miles, L., Ortega-Huerta, M.A., Peterson, A.T., Phillips, O.L. & Williams, S.E. (2004) Extinction risk from climate change. *Nature*, **427**, 145–148.
- Walker, P.A. & Cocks, K.D. (1991) HABITAT: a procedure for modelling a disjoint environmental envelope for a plant or animal species. *Global Ecology and Biogeography Letters*, **1**, 108–118.
- Waring, R.H. & Franklin, J.F. (1979) Evergreen coniferous forests of the Pacific Northwest. *Science*, **204**, 1380–1386.
- Willmott, C.J., Rowe, C.M. & Mintz, Y. (1985) Climatology of the terrestrial seasonal water cycle. *Journal of Climatology*, **5**, 589–606.
- Woodward, F.I. & Beerling, D.J. (1997) The dynamics of vegetation change: health warnings for equilibrium 'dodo' models. *Global Ecology and Biogeography Letters*, **6**, 413–418.
- Zaniewski, A.E., Lehmann, A. & Overton, J.M.C. (2002) Predicting species spatial distributions using presence-only data: a case study of native New Zealand ferns. *Ecological Modelling*, **157**, 261–280.

#### BIOSKETCHES

**Daniel Gavin** is a postdoctoral associate in the Department of Plant Biology at the University of Illinois, Champaign-Urbana, IL. He is interested in Quaternary palaeoecology, biogeography, fire history and forest ecology.

**Feng Sheng Hu** is an associate professor in the Departments of Plant Biology and Geology at the University of Illinois. He is interested in climatic change and ecosystem response.